Received: 24 April 2023 | Revised: 5 November 2023 | Accepted: 12 November 2023

DOI: 10.1002/ca.24125

COMMUNICATION

CLINICAL ANATOMY WILEY

Definition and anatomical description of the left atrial appendage neck

Jakub Batko[1,2,3,4] | Rafał Jakiel[1] | Agata Krawczyk-Ożóg[1,5] | Radosław Litwinowicz[2,3,6] | Jakub Hołda[1] | Stanisław Bartuś[5] | Krzysztof Bartuś[4] | Mateusz K. Hołda[1,7,8] | Małgorzata Konieczyńska[7,9]

[1]HEART—Heart Embryology and Anatomy Research Team, Department of Anatomy, Jagiellonian University Medical College, Cracow, Poland

[2]CAROL—Cardiothoracic Anatomy Research Operative Lab, Department of Cardiovascular Surgery and Transplantology, Institute of Cardiology, Jagiellonian University Medical College, Krakow, Poland

[3]Thoracic Research Centre, Collegium Medicum, Nicolaus Copernicus University, Bydgoszcz, Poland

[4]Department of Cardiovascular Surgery and Transplantology, Institute of Cardiology, Jagiellonian University Medical College, Krakow, Poland

[5]Department of Cardiology and Cardiovascular Interventions, University Hospital in Cracow, Krakow, Poland

[6]Department of Cardiac Surgery, Regional Specialist Hospital, Grudziądz, Poland

[7]Department of Diagnostic Medicine, John Paul II Hospital in Kraków, Krakow, Poland

[8]Division of Cardiovascular Sciences, The University of Manchester, Manchester, UK

[9]Department of Thromboembolic Diseases, Jagiellonian University Medical College, Cracow, Poland

Correspondence
Mateusz K. Hołda, HEART—Heart Embryology and Anatomy Research Team, Department of Anatomy Jagiellonian, University Medical College, Kopernika 12, 31-034 Krakow, Poland.
Email: mkh@onet.eu

Funding information
Narodowe Centrum Badań i Rozwoju, Grant/Award Number: LIDER/7/0027/L-10/18/NCBR/2019; Narodowe Centrum Nauki, Grant/Award Number: UMO-2019/33/B/NZ5/02395; Bioethical Committee of the Jagiellonian University, Cracow, Poland, Grant/Award Numbers: 1072.6120.151.2019, 1072.6120.205.2019

Abstract

The left atrial appendage (LAA) is well known as a source of cardiac thrombus formation. Despite its clinical importance, the LAA neck is still anatomically poorly defined. Therefore, this study aimed to define the LAA neck and determine its morphometric characteristics. We performed three-dimensional reconstructions of the heart chambers based on contrast-enhanced electrocardiography–gated computed tomography scans of 200 patients (47% females, 66.5 ± 13.6 years old). The LAA neck was defined as a truncated cone-shaped canal bounded proximally by the LAA orifice and distally by the lobe origin and was present in 98.0% of cases. The central axis of the LAA neck was 14.7 ± 2.3 mm. The mean area of the LAA neck walls was 856.6 ± 316.7 mm^2. The LAA neck can be divided into aortic, arterial (the smallest), venous (the largest), and free surfaces. All areas have a trapezoidal shape with a broader proximal base. There were no statistically significant differences in the morphometric characteristics of the LAA neck between LAA types. Statistically significant differences between the sexes in the main morphometric parameters of the LAA neck were found in the central axis length and the LAA neck wall area. The LAA neck can be evaluated from computed tomography scans and their three-dimensional reconstructions. The current study provides a complex morphometric analysis of the LAA neck. The precise definition and morphometric details of the

LAA neck presented in this study may influence the effectiveness and safety of LAA exclusion procedures.

KEYWORDS
atrial appendage, atrial fibrillation, cardiac surgical procedures, heart atria

1 | INTRODUCTION

1.1 | Stroke prevention in atrial fibrillation

The incidence and prevalence of atrial fibrillation are on the rise worldwide. It is estimated that nearly one-third of the population over 40 years of age may suffer from this disease (Kornej et al., 2020). The risk of stroke in patients with atrial fibrillation is significantly increased, and the left atrial appendage (LAA) is the primary cardioembolic source of stroke (Naksuk et al., 2016; Słodowska, Szczepanek, et al., 2021; Whiteman et al., 2019). Lifelong anticoagulation therapy is recommended in patients with atrial fibrillation to prevent fatal thromboembolic complications (Steffel et al., 2021). As an alternative to pharmacotherapy, LAA exclusion procedures are performed in patients who object to anticoagulation (e.g., at increased risk of bleeding) (Hindricks et al., 2021; Steffel et al., 2021). This procedure aims to separate the LAA from the circulatory system, thereby eliminating the most common cardiac source of thrombus.

1.2 | LAA exclusion procedures

Exclusion of the LAA can be performed in several ways. The LAA can be surgically removed, sutured, or stapled (Grygier et al., 2018; Whitlock et al., 2021). On the other hand, the LAA can be occluded in minimally invasive procedures (Lariat, AtriClip) or closed with percutaneous procedures (Watchman or Amplatzer devices) (Burysz et al., 2019; Litwinowicz et al., 2021; Litwinowicz, Bartus, Kapelak, et al., 2019; Litwinowicz, Bartus, Malec-Litwinowicz, et al., 2019; Reddy et al., 2013; Toale et al., 2019). All the above procedures are performed in the LAA neck region, whose morphological feature is significant for percutaneously implanted devices. Therefore, the anatomy of the LAA neck and its surrounding area may influence the safety and efficacy of LAA closure procedures (Batko et al., 2022).

1.3 | The clinical implication of the LAA neck

The LAA neck is one of the most clinically essential parts of the appendage. It is located between the LAA orifice and the LAA main lobe and clinically serves as the site of LAA closure or implantation of occluding devices. Despite the tremendous clinical importance of the LAA neck, its anatomical description is still inadequate. Therefore, this study aimed to provide the first complex morphological and morphometric description of the LAA neck and to discuss the clinical relevance of the individual components of the LAA neck. Providing such an anatomical description may increase clinicians' knowledge of the complex anatomy of this region and contribute to the effectiveness and safety of LAA exclusion procedures.

2 | MATERIALS AND METHODS

This study was approved by the Bioethical Committee of the Jagiellonian University, Cracow, Poland (nos. 1072.6120.205.2019 and 1072.6120.151.2019). The study protocol conforms to the ethical guidelines of the 1975 Declaration of Helsinki.

2.1 | Study population

We analyzed a set of consecutive cardiac contrast-enhanced electrocardiogram-gated computed tomography (CT) scans performed at the Department of Cardiology and Cardiovascular Interventions, University Hospital in Cracow, for coronary artery disease evaluation. The exclusion criteria were low-quality CT images and any significant valvular or structural heart disease in the patient's history or revealed during hospitalization. As a result, the study included 200 adult patients (47.0% females, mean age 66.5 ± 13.6 years old) for further evaluation.

2.2 | Cardiac CT protocol

The CT was performed in the sinus rhythm using a 64-row dual-source scanner (Aquilion 64, Toshiba Medical Systems, Tokyo, Japan) during deep inspiration breath-hold. Depending on physician recommendation, 10 or 40 mg of propranolol or 40 mg of verapamil was administered to patients with heart rates over 70 bpm before the procedure. The imaging parameters for CT were 100–120 kV tube voltage and 350–400 mA effective tube current. The collimation was 2 × 32 × 0.6 mm, and the temporal resolution was 165 ms. The time of the contrast agent's arrival to the ascending aorta was established at the level of the tracheal bifurcation with the test bolus method in which the 15 mL of contrast agent followed by 20 mL of saline was infused. Then, the contrast agent at a dose of 1.0 mL/kg and 40 mL saline chaser was injected at a rate of 5.5 mL/s each. In the test bolus, the acquisition delay was the time of maximum density of the ascending aorta with an additional 6 s delay. Images were reconstructed with a B26f and B46f kernel and an image matrix of 512 × 512 pixels. A multiphase reconstruction (from 10% to 100%) was done, and the 70% phase was evaluated as left ventricle end-diastole. All CT scans were analyzed on a dedicated workstation (Dell, USA). Three-dimensional reconstructions of the left atrium together with LAA and left ventricle, aortic root, and coronary vessels were created using volume-rendering and segmentation techniques using Mimics Innovation Suite 22 software (Materialise, Plymouth, MI, USA) in a predefined phase. Manual and semi-automatic methods of segmentation were used. Raw data and visualizations were further morphologically and morphometrically analyzed using virtual calipers.

2.3 | Morphological and morphometrical analyses

The following definitions were implemented in this study to describe the LAA morphology. The LAA body is divided into the neck and lobe (Figure 1). The LAA lobe is the central part of the LAA body where pectinate muscles are present. The LAA lobe has an irregular external shape that could be divided into different types (Słodowska, Szczepanek, et al., 2021; Wang et al., 2010). The LAA neck is defined as a truncated cone-shaped canal, bounded proximally by the LAA orifice and distally by the lobe origin (lobe entry). The LAA neck was morphologically evaluated with particular emphasis on its proximity to the surrounding heart structures. Based on the position concerning neighboring structures, the neck can be divided into four surfaces (Figure 2):

1. Venous—adjacent to the left superior pulmonary vein ostium (or left common pulmonary vein ostium if present),
2. Aortic—adjacent to aortic root (left coronary aortic sinus and left coronary artery trunk), bounded by the superior margin of the left superior pulmonary vein ostium (or left common pulmonary vein ostium if present) and left coronary artery bifurcation.
3. Arterial—adjacent to the left circumflex artery (periappendicular course of the left circumflex artery).
4. And free surface—located between venous and arterial surface, bounded by the end of periappendicular course of the left circumflex artery and the inferior margin of the left superior pulmonary vein (or left common pulmonary vein ostium if present).

The LAA orifice and lobe entry diameters (anteroposterior and transverse) were measured. The length of the LAA neck central axis, as well as the length of each neck surface, were measured. The length of the boundaries between surfaces was also measured. Proximal (at the LAA orifice) and distal (at the lobe entrance) heights of the LAA neck surfaces were also obtained (Figure 3). The surface area of the neck walls was calculated.

2.4 | Statistical analyses

The data was analyzed using IBM SPSS Statistics 28.0 (Predictive Solutions, Pittsburgh, PA, USA). Categorical variables are presented as numbers (n) or percentages. Quantitative variables are presentation as mean with standard deviation. The normal distribution was explored with the Shapiro–Wilk test. Differences between customarily distributed quantitative parameters were assessed with the student t-test, and non-normally distributed quantitative data was checked using the Mann–Whitney U test. The differences between categorical variables were determined using the chi-square test of independence. Differences between more than two groups were also assessed. For normally distributed data, a one-way analysis of variance (one-way ANOVA) was used with Tukey's post hoc test to determine if ANOVA results were statistically significant. For non-normally distributed data, Kruskal and Wallis's test was used with Dunn's post hoc test to determine if their test results were statistically significant. For categorical variables, the chi-square test of independence was used. Correlations were checked using rho Spearman correlation (two-tailed, $\alpha = 0.05$, $\beta = 0.2$). In the results, post hoc tests p-value of direct group comparison was presented. In tables, ANOVA simultaneous group comparison p-values were presented. A p-value <0.05 was considered significant.

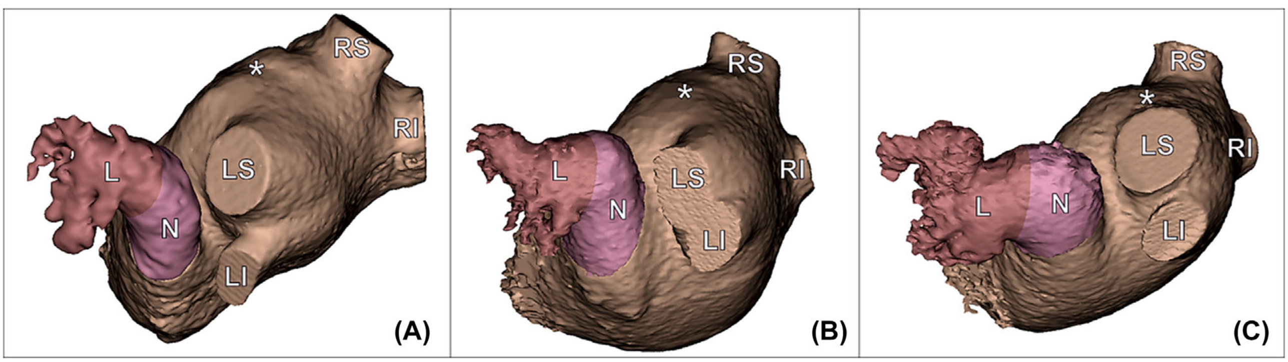

FIGURE 1 Three-dimensional reconstructions segmented from contrast-enhanced computed tomography of hearts showing a left lateral view of the left atrial area. The left atrial appendage subdivision into the neck (N) and lobe (L) is visible. *, left atrial roof; LI, left inferior pulmonary vein; LS, left superior pulmonary vein; RI, right inferior pulmonary vein; RS, right superior pulmonary vein.

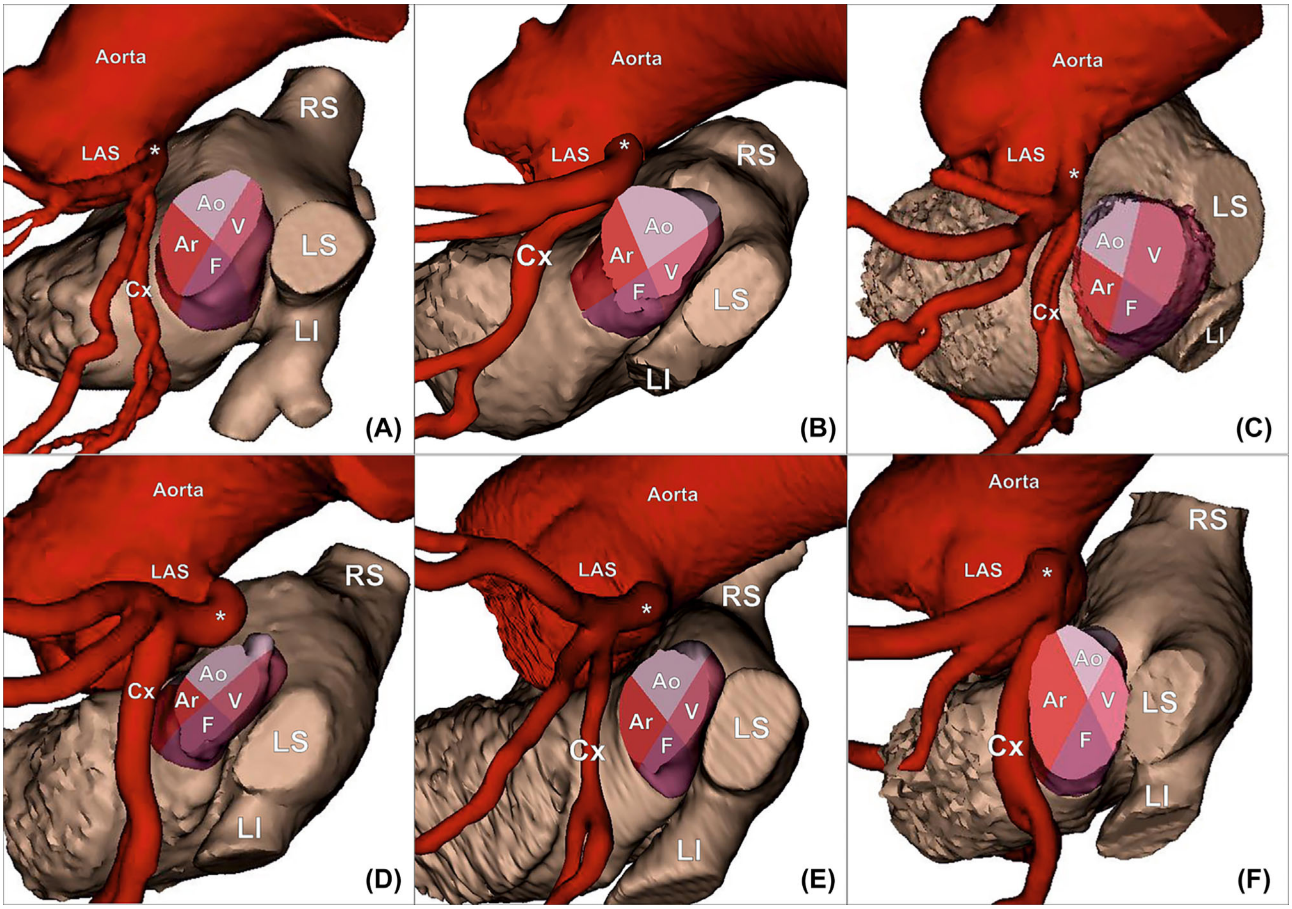

FIGURE 2 Three-dimensional reconstructions segmented from contrast-enhanced computed tomography of hearts showing a left lateral view of the left atrial area. The left atrial appendage body is removed from the neck to show the left atrial appendage neck division into four surfaces: venous (V), aortic (Ao), arterial (Ar), and free surface (F). *, left coronary artery trunk; Cx, left circumflex artery; LAS, left coronary aortic sinus; LI, left inferior pulmonary vein; LS, left superior pulmonary vein; RS, right superior pulmonary vein.

3 | RESULTS

3.1 | Morphometric parameters of the LAA neck

The LAA neck was present in 98.0% of cases, and in the remaining 2.0%, the LAA orifice connected the left atrium directly to the pectinated body of the LAA (no visible neck). The size of the LAA orifice was significantly larger than the LAA lobe entrance (anteroposterior diameter: 18.0 ± 4.3 mm vs. 17.1 ± 4.1 mm, $p = 0.024$; the transverse diameter: 26.3 ± 5.4 mm vs. 17.7 ± 3.9 mm, $p < 0.001$). In 71.9% of hearts, the LAA orifice may be classified as oval, and the remaining 28.1% as round. The central axis of the LAA neck was 14.7 ± 2.3 mm. The mean area of the LAA neck surface was 856.6 ± 316.7 mm^2. The neck was divided into four surfaces: venous, aortic, arterial, and free. Table 1 shows the measurements performed and the comparison of surface morphometry. The venous surface of the LAA neck is the largest (the largest surface wall area), followed by the aortic, free, and arterial surfaces (Table 1, $p < 0.001$). It is also the longest among all surfaces (venous > free > aortic > arterial) (Table 1, $p < 0.001$). All surfaces are trapezoidal, with the proximal base wider than the distal base (Table 1). The borders between the surfaces were also measured, with the longest dimension for the aortic-venous boundary (23.8 ± 5.8 mm), followed by the venous-free surface boundary (17.2 ± 7.4 mm), the aortic-arterial surface boundary (12.1 ± 4.0 mm) and the arterial—free surface boundary (6.1 ± 3.1 mm) ($p < 0.001$). The size comparison of the LAA neck surfaces, regarding the shape of the LAA orifice (round vs. oval), showed statistically significant differences only in aortic proximal surface height ($p = 0.002$) and free surface proximal ($p = 0.026$) and distal heights ($p = 0.004$) (larger in round orifices, for details see Table A1). In the studied population, cauliflower type was present in 38.5% of patients, chicken wing in 32.0%, and arrowhead in 29.5%. There were no statistically significant differences in the LAA neck morphometric characteristics between LAA types (all $p > 0.05$).

3.2 | Age and sex differences in the LAA neck morphometry

Statistically significant differences between the sexes were observed in the main morphometric parameters of the LAA, with larger values

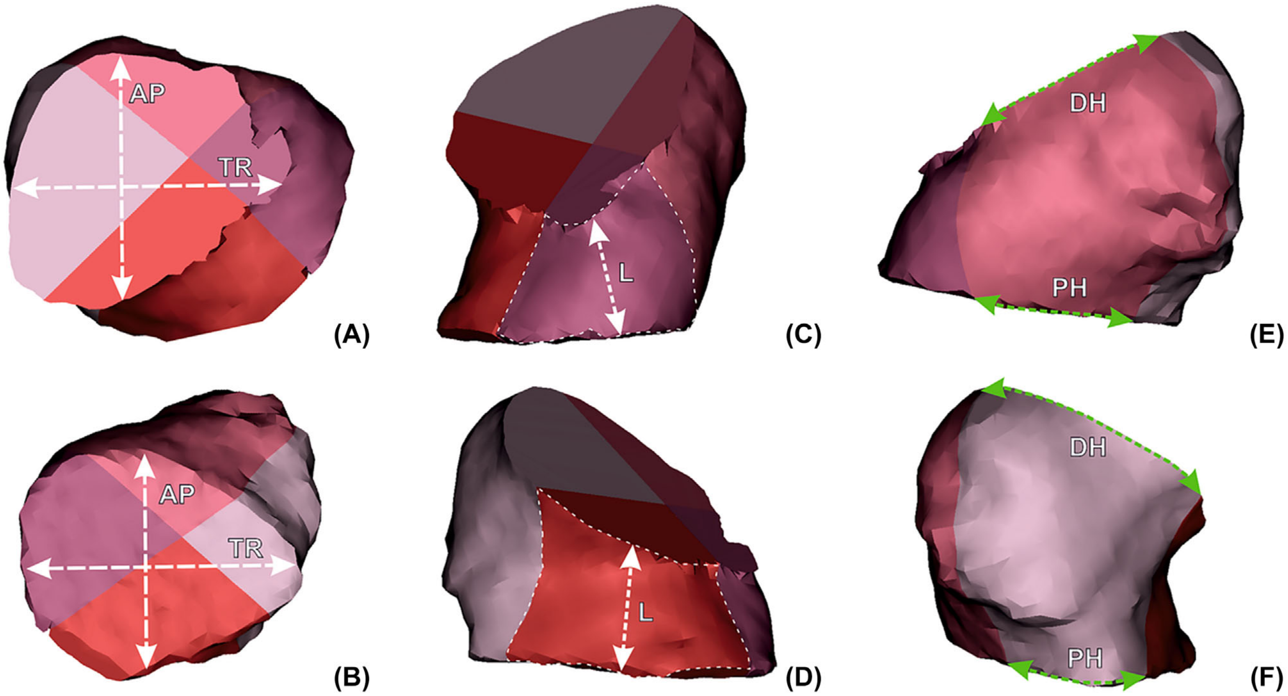

FIGURE 3 Three-dimensional reconstructions segmented from contrast-enhanced computed tomography of the heart showing the left atrial appendage neck in different views. The measurement sites are marked. (A) left atrial appendage orifice anteroposterior and transverse diameters; (B) lobe entry anteroposterior and transverse diameters; (C) and (D) neck surface length (L); (E) and (F) proximal (at LAA orifice) (PH) and distal (at the lobe entrance) (DH) heights of the neck surfaces.

TABLE 1 The left atrial appendage (LAA) neck surfaces comparison (mean ± standard deviation).

Parameter	Venous surface	Aortic surface	Arterial surface	Free surface	*p*-value ANOVA
Surface length (mm)	24.1 ± 5.7	15.4 ± 4.8	6.4 ± 3.2	16.6 ± 4.2	**<0.001**
Proximal surface height (at LAA orifice) (mm)	16.4 ± 4.0	14.0 ± 5.5	17.8 ± 5.1	13.5 ± 5.9	**<0.001**
Distal surface height (at lobe entrance) (mm)	11.8 ± 3.1	13.4 ± 4.9	15.5 ± 4.6	7.3 ± 4.8	**<0.001**
Surface wall area (mm^2)	345.6 ± 129.9	232.3 ± 110.3	108.4 ± 67.2	170.3 ± 113.1	**<0.001**
Surface wall area/LAA neck wall area ratio	40.8% ± 7.1%	27.2% ± 8.7%	12.6% ± 5.7%	19.3% ± 9.5%	**<0.001**

Note: Statistically significant *p*-values bolded.

observed in men than in women: length of the central axis (males: 15.3 ± 2.2 mm vs. females: 14.0 ± 2.4 mm; $p = 0.027$) and area of the LAA neck (males: 914.3 ± 318.4 mm^2 vs. females: 795.2 ± 304.8 mm^2; $p = 0.006$). Detailed between-sex comparisons for each LAA neck surface are shown in Table A2. In addition, significant positive correlations were found between the obtained morphometric parameters and the age of the patients for the central axis length ($r = 0.22$, $p = 0.002$), LAA transverse ($r = 0.27$, $p < 0.001$), and anteroposterior ($r = 0.33$, $p < 0.001$) orifice diameters, LAA transverse lobe entrance diameter ($r = 0.25$, $p < 0.001$), as well as with area of the LAA neck surface ($r = 0.24$, $p < 0.001$), LAA neck free surface area ($r = 0.21$, $p = 0.003$) and LAA neck venous surface area ($r = 0.20$, $p = 0.005$). No other statistically significant differences or correlations were found (all $p > 0.05$).

4 | DISCUSSION

4.1 | The LAA in the context of the left atrial anatomy

As previously described, several parts can be seen in the left atrium, including the body, vestibule, septal portion, venous compartment, and appendage (Anderson et al., 2000; Ho et al., 2012; Wang et al., 1995). Apart from the atrial appendage, with a well-defined orifice, the other atrial modules do not have clear boundaries. An excellent tool for left atrial anatomy analysis is virtual dissection, which utilizes reconstructions from cardiac CT scans and thus allows the study of three-dimensional cardiac anatomy in great detail and proper anatomical position (Mori et al., 2019). Its embryological origin should be mentioned to understand the LAA anatomy better. The LAA development begins in Carnegie stage 11 when the atrial appendages and apical ventricular components balloon as a result of radial growth of the developing heart. The pectinate muscles, visible from stage 14, expands in stage 18, further developing both atrial appendages. Its further size and pectinate muscle development can be observed during Carnegie stage 23 (Hikspoors et al., 2022).

4.2 | The lack of a definition of the LAA neck

Although the LAA anatomy appears thoroughly known (Dudkiewicz et al., 2021; Roberts et al., 2019; Slodowska et al., 2022; Słodowska, Hołda, et al., 2021; Słodowska, Szczepanek, et al., 2021), the LAA neck has not been well defined or explored. The growing clinical importance of the LAA as a common source of thrombus formation and the introduction of various LAA exclusion techniques into daily clinical practice forced us to provide a detailed morphological description of the most proximal part of the LAA—the neck region (Naksuk et al., 2016; Słodowska, Szczepanek, et al., 2021; Whiteman et al., 2019). The LAA neck is clinically where occlusion and closure devices are implanted. In the past, the LAA neck has been defined indirectly as the portion of either the LAA body or the left atrium. It has been described as a region where occluding devices are placed, a junction between the orifice, landing zone, and lobar region (Beigel et al., 2014; Grygier et al., 2018; Naksuk et al., 2016). The term "LAA neck" has also been mentioned in a few recent anatomical publications without clearly defining this structure (Slodowska et al., 2022; Whiteman et al., 2019).

4.3 | The precise anatomical definition of the LAA neck

Our study is the first to define the LAA neck precisely and deliver data on its morphological features and subdivision into potentially clinically essential surfaces. The anatomic definition of the LAA neck provided in the current study incorporates the region defined by clinicians as the LAA landing zone—a crucial region of the heart for all LAA exclusion procedures (Batko et al., 2022; Grygier et al., 2018; Hindricks et al., 2021; Naksuk et al., 2016; Wang et al., 2010). Greater knowledge of the LAA anatomy may contribute to more efficient and safer performance of various procedures in this essential cardiac area. Better awareness of the LAA neck anatomy may also contribute to a more accurate choice of used LAA exclusion technique or suitable LAA occlusion device, reducing the risk of complications and peri-device leaks (Burysz et al., 2019; Litwinowicz et al., 2021; Litwinowicz, Bartus, Kapelak, et al., 2019; Litwinowicz, Bartus, Malec-Litwinowicz, et al., 2019; Reddy et al., 2013; Toale et al., 2019; Whitlock et al., 2021). Providing a clear definition of the studied region may also facilitate communication between clinicians and researchers regarding a detailed description of complications that may occur during LAA exclusion procedures. Nowadays, specific complications related to the LAA exclusion, especially those related to the destruction of adjacent structures, are hard to evaluate because of the lack of proper terminology to describe damage precise localization. This significant obstacle can now be removed by reporting damages occurring in particular LAA areas defined as LAA neck surfaces.

4.4 | The origin of the subdivision of the LAA neck

The subdivision of the LAA neck into surfaces is based on the presence of clinically essential structures near each surface. The aortic surface is adjacent to the left coronary aortic sinus and trunk of the left coronary artery. It is separated from the pulmonary valve root by the apex of the left ventricular summit, the region of idiopathic ventricular arrhythmias (Yamada et al., 2010). The arterial surface of the LAA neck borders major coronary vessels from the epicardial side: the left circumflex coronary artery and great cardiac vein (Kassem et al., 2021). Therefore, the arterial surface borders the accessible and inaccessible part of the left ventricular summit (Kuniewicz et al., 2021). From the endocardial side, it is separated from the mitral valve annulus by the LAA isthmus, which is a potential ablation target (Hołda et al., 2017). Near the free surface of the LAA neck, the vein or ligament of Marshall may be present, which is known to be an essential site of abnormal cardiac electrical activity (He et al., 2021; Żabówka et al., 2020). From the endocardial side, the free surface of the LAA neck is separated from the mitral valve annulus by the mitral isthmus (Hołda et al., 2017). We observed some deformations of the left atrial wall in this region, which should be further analyzed and described. The venous surface is adjacent to the left pulmonary veins, and as previously reported, the left atrial ridge (coumadin ridge) may be present in this area in 60% of hearts (Piątek-Koziej et al., 2020).

4.5 | The clinical significance of the LAA neck

The size of the LAA neck may influence the course of procedures aimed at excluding the LAA. The manufacturers of the Watchman and Amplatzer devices define the minimum central axis of the LAA neck for performing LAA occlusion as at least 10 mm (Grygier et al., 2018). As shown in the current study, the mean length of the LAA neck central axis is above 14 mm, but in 4.5% of all cases studied, the length was <10 mm, making these hearts unsuitable for LAA occlusion devices implantation. However, the measured arterial surface length was 6.4 ± 3.2 mm. The influence of each wall parameter should be further investigated to evaluate its impact on the effectiveness of the LAA closure procedure and potential complications. Other closure methods may be more appropriate for patients with shorter central axis of the LAA neck (Lee & Hanke, 2022; Litwinowicz et al., 2021; Litwinowicz, Bartus, Kapelak, et al., 2019; Toale et al., 2019). One of the most dangerous complications associated with LAA exclusion procedures is damage or occlusion of the left circumflex coronary artery (Batko et al., 2022; Kuzmin et al., 2021). Some of the specific arrangements of coronary vessels within the LAA isthmus, localized inferiorly

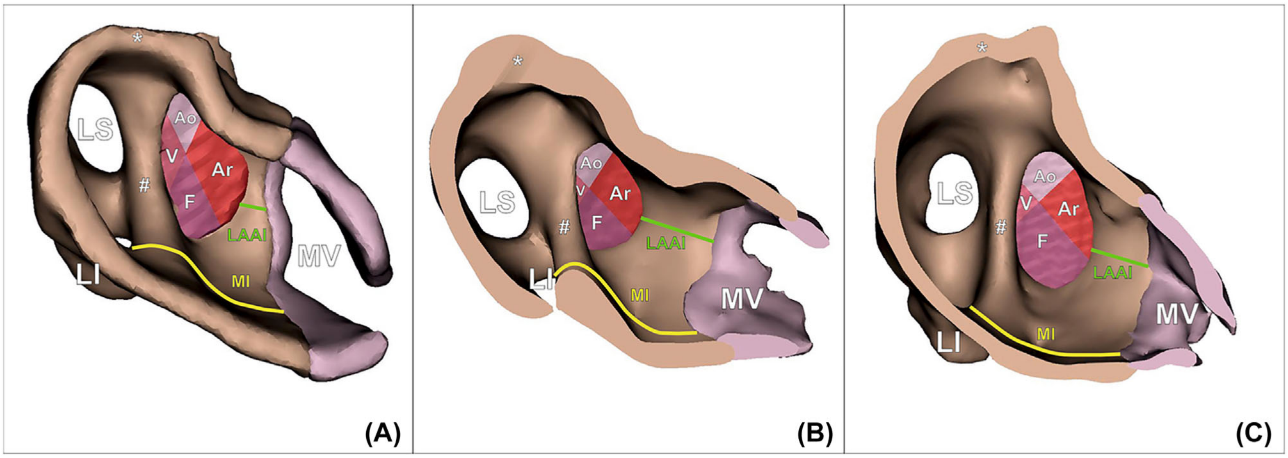

FIGURE 4 Three-dimensional endocardial reconstruction segmented from contrast-enhanced computed tomography of the heart showing the left atrial appendage neck concerning mitral isthmus (MI—yellow) and left atrial appendage isthmus (LAAI—green). Venous (V), aortic (Ao), arterial (Ar), and free surface (F). #, left atrial ridge; *, left atrial roof; LI, left inferior pulmonary vein; LS, left superior pulmonary vein; MV, mitral valve.

to the arterial surface, may predispose to severe vascular injury (Batko et al., 2022; Hołda, Hołda, et al., 2018; Hołda, Koziej, et al., 2018). Additionally, the studied region is of great interest to electrophysiologists, as the mitral isthmus and LAA isthmus, where ablations are performed, are adjacent to the LAA ostium and neck (Hołda et al., 2017). Relation between the mitral and LAA isthmus and the LAA neck are presented in Figure 4. Moreover, the arterial surface of the LAA neck was found to be the smallest among all areas of the LAA neck, which may further contribute to lacerations located near the base of the LAA (Lee & Hanke, 2022). The LAA itself can be divided into several types (Wang et al., 2010). The most recent classification proposes three LAA types based on the shape of its body: chicken wing, cauliflower, and arrowhead (Słodowska, Szczepanek, et al., 2021). Notably, the current research found that there are no statistically significant differences or correlations regarding the LAA type and the LAA neck morphometry. Only isolated differences were found in the LAA neck dimensions between hearts with round versus oval LAA orifices.

4.6 | Study limitations

Several significant limitations of this study should be stated. First, the current study is a single-center, retrospective CT scan analysis aimed at one ethnic group (Caucasians). Second, it was performed on a relatively old population. Therefore, further studies should focus on younger patients. Moreover, the used three-dimensional segmentation tool (Mimics Innovation Suite 22, Materialise) is different from a typical clinical tool used in everyday practice but an expensive software with high hardware requirements that demand high experience in operation. Furthermore, some functional anatomy studies should be performed to show LAA neck morphology behavior during the cardiac cycle. Additionally, future research should be performed to indicate atrial fibrillation's impact on LAA neck morphology. Finally, additional analysis of the LAA neck wall thickness performed on cadaveric material may give further essential data on this heart region regarding LAA exclusion procedures. Despite these limitations, the current study delivers a complex morphometrical analysis of the LAA neck that may have clinical significance for LAA exclusion procedures.

5 | CONCLUSIONS

The neck of the LAA is the smooth-walled, truncated cone-shaped channel located between its pectinated component and the body of the left atrium. The LAA neck can be evaluated based on cardiac CT scans and three-dimensional reconstructions. Based on its position concerning neighboring structures, the LAA neck can be divided into four surfaces: venous, aortic, arterial, and free surface. Significant differences in surfaces' morphometry are observed, with the venous surface being the largest and arterial the smallest part of the LAA neck. The neck of the LAA neighbors with several crucial heart structures, including the left superior pulmonary vein, aortic root (left aortic sinus), left coronary artery trunk, and left circumflex coronary artery with an accompanying great cardiac vein. Precise definition and morphometrical details of the LAA neck that were introduced in this study may influence the effectiveness and safety of LAA exclusion procedures.

ACKNOWLEDGMENTS

This study was approved by the Bioethical Committee of the Jagiellonian University, Cracow, Poland (no. 1072.6120.205.2019 and 1072.6120.151.2019 approved in 2019). The study protocol conforms to the ethical guidelines of the 1975 Declaration of Helsinki.

FUNDING INFORMATION

This research was supported by National Centre for Research and Development, Poland (LIDER/7/0027/L-10/18/NCBR/2019) and the National Science Centre, Poland (UMO-2019/33/B/NZ5/02395), supported the research. The funding sources were not involved in the study's design, data collection, analysis, interpretation, report writing, or the decision to submit the article for publication.

ORCID

Jakub Batko https://orcid.org/0000-0002-5329-5856
Agata Krawczyk-Ożóg https://orcid.org/0000-0001-7691-8174
Mateusz K. Hołda https://orcid.org/0000-0001-5754-594X

REFERENCES

Anderson, R. H., Ho, S. Y., & Becker, A. E. (2000). Anatomy of the human atrioventricular junctions revisited. *The Anatomical Record*, *260*, 81–91. https://doi.org/10.1002/1097-0185(20000901)260:1<81::AID-AR90>3.0.CO;2-3

Batko, J., Rams, D., Filip, G., Bartoszcze, A., Kapelak, B., Bartuś, K., & Litwinowicz, R. (2022). Left atrial appendage morphology and course of the circumflex artery: Anatomical implications for left atrial appendage occlusion procedures. *Innovations: Technology and Techniques in Cardiothoracic and Vascular Surgery*, *17*, 424–429. https://doi.org/10.1177/15569845221128569

Beigel, R., Wunderlich, N. C., Siew, Z., Ho, Y., Arsanjani, R., & Siegel, R. J. (2014). The left atrial appendage: Anatomy, function, and noninvasive. *Evaluation*, *7*, 1251–1265.

Burysz, M., Litwinowicz, R., Bryndza, M., Skowronek, R., Ogorzeja, W., & Bartus, K. (2019). Percutaneous left atrial appendage closure using the LAmbre device. First clinical results in Poland. *Advances in Interventional Cardiology*, *15*, 251–254. https://doi.org/10.5114/aic.2019.86019

Dudkiewicz, D., Słodowska, K., Jasińska, K. A., Dobrzynski, H., & Hołda, M. K. (2021). The clinical anatomy of the left atrial structures used as landmarks in ablation of arrhythmogenic substrates and cardiac invasive procedures. *Translational Research in Anatomy*, *23*, 1–5. https://doi.org/10.1016/j.tria.2020.100102

Grygier, M., Wojakowski, W., Smolka, G., Demkow, M., Wąsek, W., Sorysz, D., Kralisz, P., Bartuś, K., Sukiennik, A., Pracoń, R., Witkowski, A., Kowalski, O., & Legutko, J. (2018). Left atrial appendage occlusion: Consensus document of association of cardiovascular interventions and heart rhythm section of polish cardiac society. *Kardiologia Polska*, *76*, 677–697. https://doi.org/10.5603/KP.a2018.0057

He, B., Wang, X., Zhao, F., Guo, T., Po, S. S., & Lu, Z. (2021). The ligament of Marshall and arrhythmias: A review. *Pacing and Clinical Electrophysiology*, *44*, 792–799. https://doi.org/10.1111/pace.14071

Hikspoors, J. P. J. M., Kruepunga, N., Mommen, G. M. C., Köhler, S. E., Anderson, R. H., & Lamers, W. H. (2022). A pictorial account of the human embryonic heart between 3.5 and 8 weeks of development. *Communications Biology*, *5*, 226. https://doi.org/10.1038/s42003-022-03153-x

Hindricks, G., Potpara, T., Dagres, N., Arbelo, E., Bax, J. J., Blomström-Lundqvist, C., Boriani, G., Castella, M., Dan, G.-A., Dilaveris, P. E., Fauchier, L., Filippatos, G., Kalman, J. M., La Meir, M., Lane, D. A., Lebeau, J.-P., Lettino, M., Lip, G. Y. H., Pinto, F. J., … ESC Scientific Document Group. (2021). 2020 ESC Guidelines for the diagnosis and management of atrial fibrillation developed in collaboration with the European Association for Cardio-Thoracic Surgery (EACTS). *European Heart Journal*, *42*, 373–498. https://doi.org/10.1093/eurheartj/ehaa612

Ho, S. Y., Cabrera, J. A., & Sanchez-Quintana, D. (2012). Left atrial anatomy revisited. *Circulation. Arrhythmia and Electrophysiology*, *5*, 220–228. https://doi.org/10.1161/CIRCEP.111.962720

Hołda, M. K., Hołda, J., Strona, M., Koziej, M., & Klimek-Piotrowska, W. (2018). Blood vessels and myocardial thickness within the left atrial appendage isthmus line. *Clinical Anatomy*, *31*, 1024–1030. https://doi.org/10.1002/ca.23242

Hołda, M. K., Koziej, M., Hołda, J., Tyrak, K., Piątek, K., Bolechała, F., & Klimek-Piotrowska, W. (2017). Anatomic characteristics of the mitral isthmus region: The left atrial appendage isthmus as a possible ablation target. *Annals of Anatomy*, *210*, 103–111. https://doi.org/10.1016/j.aanat.2016.11.011

Hołda, M. K., Koziej, M., Hołda, J., Tyrak, K., Piątek, K., Krawczyk-Ożóg, A., & Klimek-Piotrowska, W. (2018). Spatial relationship of blood vessels within the mitral isthmus line. *EP Europace*, *20*, 706–711. https://doi.org/10.1093/europace/euw423

Kassem, M. W., Lake, S., Roberts, W., Salandy, S., & Loukas, M. (2021). Cardiac veins, an anatomical review. *Translational Research in Anatomy*, *23*, 1–10. https://doi.org/10.1016/j.tria.2020.100096

Kornej, J., Börschel, C. S., Benjamin, E. J., & Schnabel, R. B. (2020). Epidemiology of atrial fibrillation in the 21st century: Novel methods and new insights. *Circulation Research*, *127*, 4–20. https://doi.org/10.1161/CIRCRESAHA.120.316340

Kuniewicz, M., Baszko, A., Ali, D., Karkowski, G., Loukas, M., Walocha, J. A., & Hołda, M. K. (2021). Left ventricular summit—Concept. *Anatomical Structure and Clinical Significance. Diagnostics*, *11*, 1423. https://doi.org/10.3390/diagnostics11081423

Kuzmin, B., Staack, T., Wippermann, J., & Wacker, M. (2021). Left atrial appendage occlusion device causing coronary obstruction: A word of caution. *Journal of Cardiac Surgery*, *36*, 723–725. https://doi.org/10.1111/jocs.15222

Lee, R. J., & Hanke, T. (2022). The strengths and weaknesses of left atrial appendage ligation or exclusion (LARIAT, AtriaClip, surgical suture). *Interventional Cardiology Clinics*, *11*, 205–217. https://doi.org/10.1016/j.iccl.2022.01.001

Litwinowicz, R., Bartus, M., Kapelak, B., Suwalski, P., Lakkireddy, D., Lee, R. J., & Bartus, K. (2019). Reduction in risk of stroke and bleeding after left atrial appendage closure with LARIAT device in patients with increased risk of stroke and bleeding: Long term results. *Catheterization and Cardiovascular Interventions*, *94*, 837–842. https://doi.org/10.1002/ccd.28187

Litwinowicz, R., Bartus, M., Malec-Litwinowicz, M., Michalski, M., Banaszkiewicz, K., Kapelak, B., Lakkireddy, D., & Bartus, K. (2019). Left atrial appendage occlusion for secondary stroke prevention in patients with atrial fibrillation: Long-term results. *Cerebrovascular Diseases*, *47*, 188–195. https://doi.org/10.1159/000500850

Litwinowicz, R., Burysz, M., Mazur, P., Kapelak, B., Bartus, M., Lakkireddy, D., Lee, R. J., Malec-Litwinowicz, M., & Bartus, K. (2021). Endocardial versus epicardial left atrial appendage exclusion for stroke prevention in patients with atrial fibrillation: Midterm follow-up. *Journal of Cardiovascular Electrophysiology*, *32*, 93–101. https://doi.org/10.1111/jce.14802

Mori, S., Tretter, J. T., Spicer, D. E., Bolender, D. L., & Anderson, R. H. (2019). What is the real cardiac anatomy? *Clinical Anatomy*, *32*, 288–309. https://doi.org/10.1002/ca.23340

Naksuk, N., Padmanabhan, D., Yogeswaran, V., & Asirvatham, S. J. (2016). Left atrial appendage: Embryology, anatomy, physiology, arrhythmia and therapeutic intervention. *Journal of American College of Cardiology*, *2*(4), 403–412.

Piątek-Koziej, K., Hołda, J., Tyrak, K., Bolechała, F., Strona, M., Koziej, M., Lis, M., Jasińska, K. A., & Hołda, M. K. (2020). Anatomy of the left atrial ridge (coumadin ridge) and possible clinical implications for cardiovascular imaging and invasive procedures. *Journal of Cardiovascular Electrophysiology*, *31*, 220–226. https://doi.org/10.1111/jce.14307

Reddy, V. Y., Möbius-Winkler, S., Miller, M. A., Neuzil, P., Schuler, G., Wiebe, J., Sick, P., & Sievert, H. (2013). Left atrial appendage closure with the watchman device in patients with a contraindication for oral anticoagulation. *Journal of the American College of Cardiology*, *61*, 2551–2556. https://doi.org/10.1016/j.jacc.2013.03.035

Roberts, W., Salandy, S., Mandal, G., Holda, M. K., Tomaszewksi, K. A., Gielecki, J., Tubbs, R. S., & Loukas, M. (2019). Across the centuries:

Piecing together the anatomy of the heart. *Translational Research in Anatomy*, *17*, 17. https://doi.org/10.1016/j.tria.2019.100051

Słodowska, K., Hołda, J., Dudkiewicz, D., Malinowska, K., Bolechała, F., Kopacz, P., Koziej, M., & Hołda, M. K. (2021). Thickness of the left atrial wall surrounding the left atrial appendage orifice. *Journal of Cardiovascular Electrophysiology*, *32*, 2262–2268. https://doi.org/10.1111/jce.15157

Słodowska, K., Szczepanek, E., Dudkiewicz, D., Hołda, J., Bolechała, F., Strona, M., Lis, M., Batko, J., Koziej, M., & Hołda, M. K. (2021). Morphology of the left atrial appendage: Introduction of a new simplified shape-based classification system. *Heart, Lung & Circulation*, *30*, 1014–1022. https://doi.org/10.1016/j.hlc.2020.12.006

Slodowska, K. M., Batko, J., Holda, J. P., Dudkiewicz, D., Koziej, M., Litwinowicz, R., Bartus, K., & Holda, M. K. (2023). Morphometrical features of left atrial appendage in the AF patients subjected to left atrial appendage closure. *Folia Morphologica*, *82*(4), 814–821. https://doi.org/10.5603/fm.a2022.0080

Steffel, J., Collins, R., Antz, M., Cornu, P., Desteghe, L., Haeusler, K. G., Oldgren, J., Reinecke, H., Roldan-Schilling, V., Rowell, N., Sinnaeve, P., Vanassche, T., Potpara, T., Camm, A. J., Heidbüchel, H., External reviewers, Lip, G. Y. H., Deneke, T., Dagres, N., … Field, M. (2021). 2021 European Heart Rhythm Association Practical Guide on the use of non-vitamin K antagonist oral anticoagulants in patients with atrial fibrillation. *Europace*, *23*, 1612–1676. https://doi.org/10.1093/europace/euab065

Toale, C., Fitzmaurice, G. J., Eaton, D., Lyne, J., & Redmond, K. C. (2019). Outcomes of left atrial appendage occlusion using the AtriClip device: A systematic review. *Interactive Cardiovascular and Thoracic Surgery*, *29*, 655–662. https://doi.org/10.1093/icvts/ivz156

Wang, K., Ho, S. Y., Gibson, D. G., & Anderson, R. H. (1995). Architecture of atrial musculature in humans. *Heart*, *73*, 559–565. https://doi.org/10.1136/hrt.73.6.559

Wang, Y., DI Biase, L., Horton, R. P., Nguyen, T., Morhanty, P., & Natale, A. (2010). Left atrial appendage studied by computed tomography to help planning for appendage closure device placement. *Journal of Cardiovascular Electrophysiology*, *21*, 973–982. https://doi.org/10.1111/j.1540-8167.2010.01814.x

Whiteman, S., Saker, E., Courant, V., Salandy, S., Gielecki, J., Zurada, A., & Loukas, M. (2019). An anatomical review of the left atrium. *Translational Research in Anatomy*, *17*, 1–8. https://doi.org/10.1016/j.tria.2019.100052

Whitlock, R. P., Belley-Cote, E. P., Paparella, D., Healey, J. S., Brady, K., Sharma, M., Reents, W., Budera, P., Baddour, A. J., Fila, P., Devereaux, P. J., Bogachev-Prokophiev, A., Boening, A., Teoh, K. H. T., Tagarakis, G. I., Slaughter, M. S., Royse, A. G., McGuinness, S., Alings, M., … Connolly, S. J. (2021). Left atrial appendage occlusion during cardiac surgery to prevent stroke. *New England Journal of Medicine*, *384*, 2081–2091. https://doi.org/10.1056/NEJMoa2101897

Yamada, T., McElderry, H. T., Doppalapudi, H., Okada, T., Murakami, Y., Yoshida, Y., Yoshida, N., Inden, Y., Murohara, T., Plumb, V. J., & Kay, G. N. (2010). Idiopathic ventricular arrhythmias originating from the left ventricular summit anatomic concepts relevant to ablation. *Circulation. Arrhythmia and Electrophysiology*, *3*, 616–623. https://doi.org/10.1161/CIRCEP.110.939744

Żabówka, A., Jakiel, M., Bolechała, F., Jakiel, R., Jasińska, K. A., & Hołda, M. K. (2020). Topography of the oblique vein of the left atrium (vein of Marshall). *Kardiologia Polska*, *78*, 688–693. https://doi.org/10.33963/KP.15318

SUPPORTING INFORMATION

Additional supporting information can be found online in the Supporting Information section at the end of this article.

How to cite this article: Batko, J., Jakiel, R., Krawczyk–Ożóg, A., Litwinowicz, R., Hołda, J., Bartuś, S., Bartuś, K., Hołda, M. K., & Konieczyńska, M. (2023). Definition and anatomical description of the left atrial appendage neck. *Clinical Anatomy*, 1–9. https://doi.org/10.1002/ca.24125